Journal of Thermal Analysis, Vol. 49 (1997) 325-334

FUNCTIONAL EVALUATION OF A LIQUID-MOLDING TWO COMPONENT COMBINATION RESIN
Study of an advanced material

B. Chowdhury

Matech Associates, 150 E.Grove Street, Scranton, PA 18510, USA

Abstract

Functional parameters contributing to the recognizable good performance of a highly crosslinked olefinic polymer based on cyclopentadiene have been evaluated by a limited range of stress decay and creep recovery from a fixed deformation over constant time periods. The experimental design for these involved a calculated stress (load) at the initial sample deformation (displacement) for determination of changes in stress in bending mode and flex creep under applied load at three constant temperature segments of 6 h each with 20 min recovery time between segments. The results have identified a behavior which is typical of interfacial orientational effect in a two-component system. Thermal conductivity, heat capacity and density at the same temperatures were measured for determination of variations in thermal diffusivity as an indication of the competing effects of densification and thermal expansion for such a system.

Static charging and polarization experiments were performed for evaluation of other desired uses of this material, in moving parts and in direct or induced voltage applications. The latter allows measurement of dynamic charge transport through the resin matrix. Calculations indicate generation of charge carriers from weak secondary bonding typical of polymer interfaces. The polarization itself consists of dipole orientation characterized by relatively high activation energy.

The intrinsic mechanical properties for this material had been determined by the manufacturer, but the performance parameters reported in this study have been determined for the first time for exploration of further uses for this material.

Keywords: generation of charge carriers, metton liquid-molding resin, static charging, stress relaxation and creep, thermal conductivity and specific heat

Introduction

Metton® liquid-molding resins (LMR's) belong to a family of highly crosslinked olefinic polymers based on polycyclopentadiene, manufactured by Hercules [1]. The manufacturing process involves in-mold metathesis polymerization to form exceptionally large rigid thermosets exhibiting the properties of engineering thermoplastics [2]. The data obtained in this study clearly indicate the thermoelastic nature of this material at elevated temperatures.

Metton®-based finished parts are considered suitable for applications in the recreational, transport, heavy equipment and lawncare markets, as well as in industrial materials handling, civil engineering and chemical-resistant entities. The core

0368–4466/97/ $ 5.00

John Wiley & Sons Limited
Chichester

property for such applications is, of course the established excellent mechanical performance of Metton.

The purpose of this study is to evaluate the functional aspects of this material in possible electronic applications at elevated temperatures.

Experimental

Thermal and thermomechanical

Although theories of rubber elasticity were established well before the availability of a wide range of synthetic high polymers, essential methodologies for studying rubber-like behavior of rigid polymers at appropriate temperatures have continued to develop, an example of which is given in Ref. [3]. In this work, short-time stress decay and creep were performed by specially designed experiments using a TA Instruments 983 DMA/9900 data analyzer [4].

Thermally activated processes are known to be controlled by diffusion and conduction of heat. Thermal conductivity was determined by a modified Differential Scanning Calorimetric (DSC) method whereby heat flow was recorded under equilibrium condition at the specified temperature and at the same time the temperature differential between the top and bottom of the sample was measured for calculation of conductivity by the following equation:

$$\lambda = qL/A(t_1 - t_2)$$

where λ – thermal conductivity/W (m K)$^{-1}$, q – steady-state heat flow/W, L – heat flow path/m, A – area of sample/m^2, $(t_1 – t_2)$ – temp. difference between the top and bottom of sample.

Heat capacity values at different temperatures were determined relative to that of a sapphire (Al_2O_3) standard by a regular DSC procedure.

Electrical

The behavior of a multi-use material like Metton® with respect to its static charge storage and decay are important design considerations for structural parts that may be subject to the influence of friction or induced voltage. The decay curve shown in Fig. 6 was obtained [5] by charging a sample measuring 6.333 cm long, 1.524 cm wide and 0.533 cm thick, with 5 KV DC voltage [6] in a Faraday cup test fixture and storing the discharge in a Keithley 617 programmable electrometer under ambient conditions of 73°F and 50% R.H.

An auxiliary technique of voltage-induced polarization [7] was used for calculation of transport properties through solid matrix. The effect of an impressed voltage field on the dielectric nature and the thermal properties of polymers in producing charge domains in the polymer is utilized in this technique for evaluation of applications that can range from determination of structure/property relationships to the practical utility of the polymer's charge storage capacity. The details of this technique for selected polymer characterization have been described previously [8, 9].

The working principles of this technique can be found in Ref. [10]. In this work, the sample was poled at 150°C, annealed for 30 min and the heating rate was 3°C min^{-1}. Depolarization current was collected every 5°C.

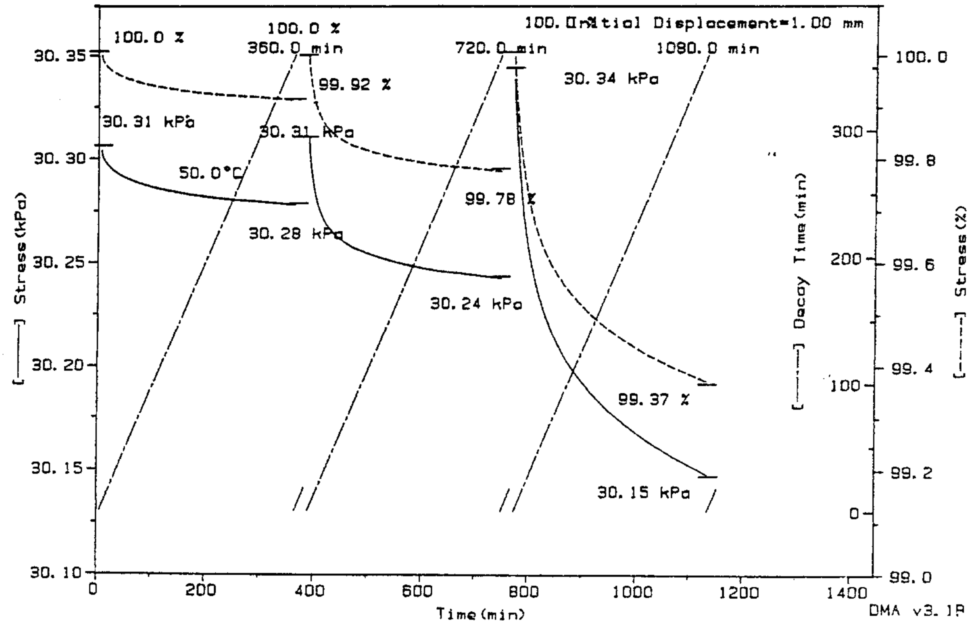

Fig. 1 Stress relaxation at 50, 75 and 100°C

Results and discussion

Figure 1 shows the short time stress decay plots in bending mode at 50°, 75° and 100°C in increasing order for 6 h at each temperature with 20 min recovery time between segments.

Changes in stress values in Table 1 clearly indicate only small changes over the entire temperature range and time period.

Table 1

t/ min	T/ °C	Stress load/	Change in stress/	*Successive strain/ **	Sample displacement/ mm
		kPa			
0	25	30.31	–	0.0689	1.0000
360	50	30.28	–0.03	0.0688	0.9990
720	75	30.24	–0.04	0.0687	0.9977
1080	100	30.15	–0.09	0.0685	0.9947

*30.31 KPa = 6.89×10^{-2}% strain for 1 mm displacement.
**As % of original.

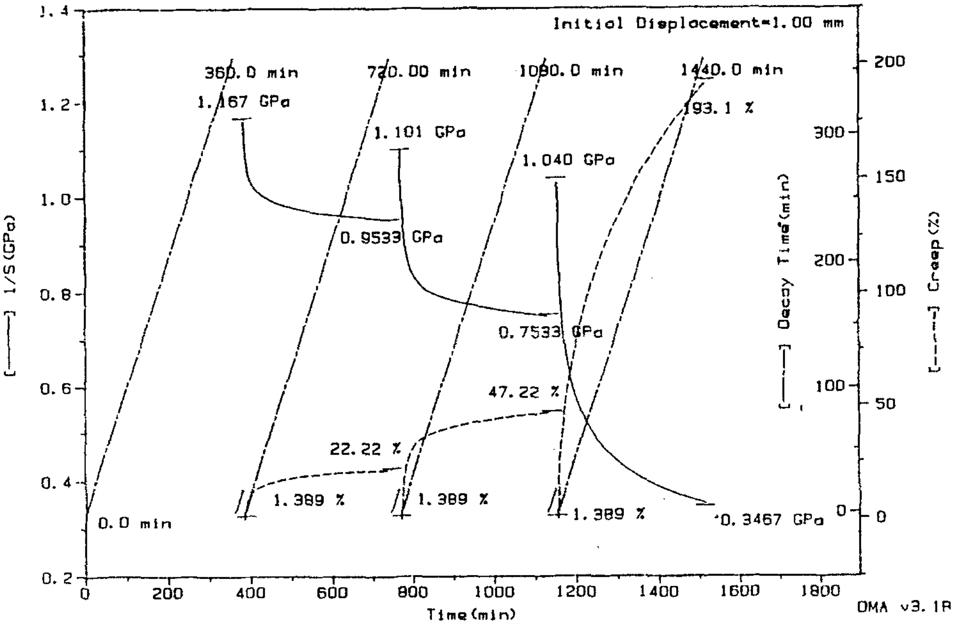

Fig. 2 Flex creep at 50, 75 and 100°C

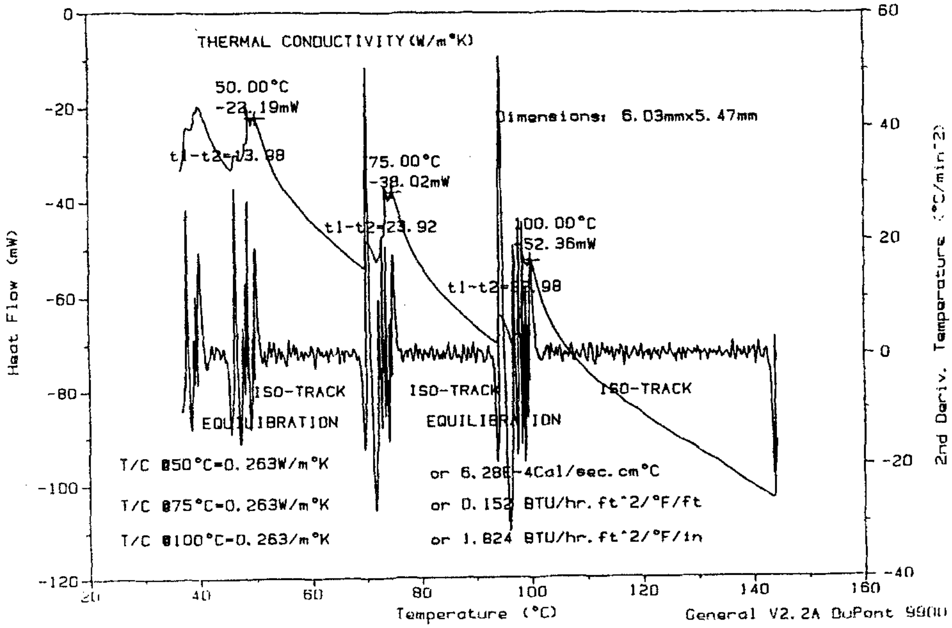

Fig. 3 Thermal conductivity at 50, 75 and 100°C

Notes

From conversion Table, 1 KPa load acting on 1 m^2 area ≅102 Kg force.

For sample area of 3.828×10^{-4} m^2 ≅3.9×10^{-2} Kg for 1 KPa load.

From instrument operating chart, 2.688 cm long and 5.51 mm thick sample at 1 mm displacement gives 6.89×10^{-2}% strain. The change in relative stress is 0.63% but a large increase in % creep is found at 100°C.

The short-time creep curves in Fig. 2 show only the elastic component, although such curves for engineering materials also include transient and steady states over long enough time period [12].

The inherent annealing effect in stress relaxation methods for non-crystalline polymers has been experimentally observed to account for the susceptibility of orientational deformation (stress) to recovery than is overall strain [12].

Evidence of interfacial orientation for Metton has been found from voltage-induced polarization in this study.

Figure 3 provides details of thermal conductivity measurement at equilibrated temperatures of 50, 75 and 100°C. The calculated corresponding heat capacity under dynamic conditions are given in Fig. 4.

Thermal diffusivity, α (cm^2 s^{-1}), was calculated by using the equation:

$$\alpha = \lambda/(\rho\times C_p)$$

where λ – thermal conductivity in J(sec cm °C$)^{-1}$, ρ – effective density in g cm^{-3}, C_p – heat capacity in J(g °C$)^{-1}$.

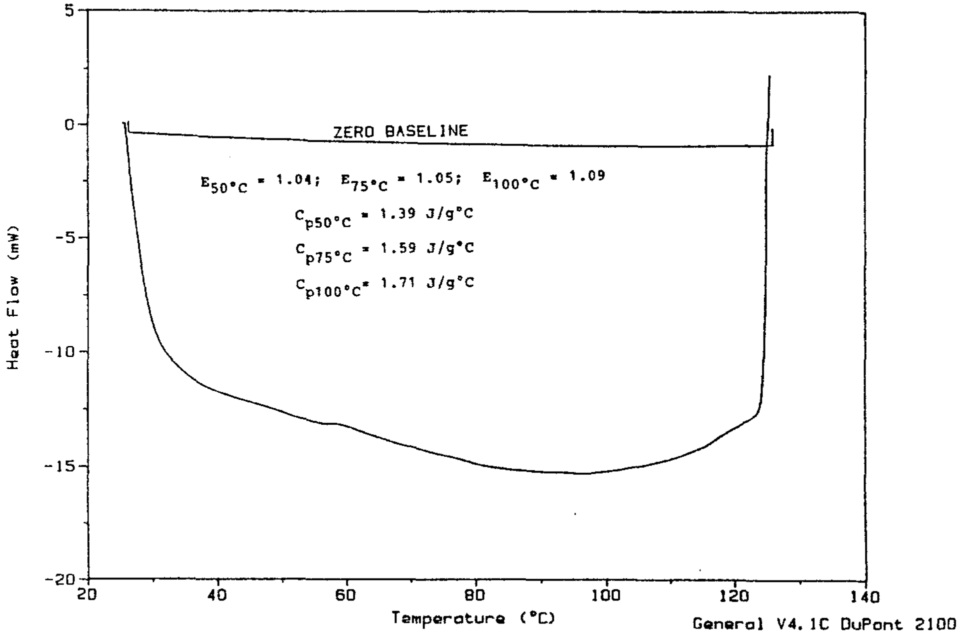

Fig. **4** Heat capacity values

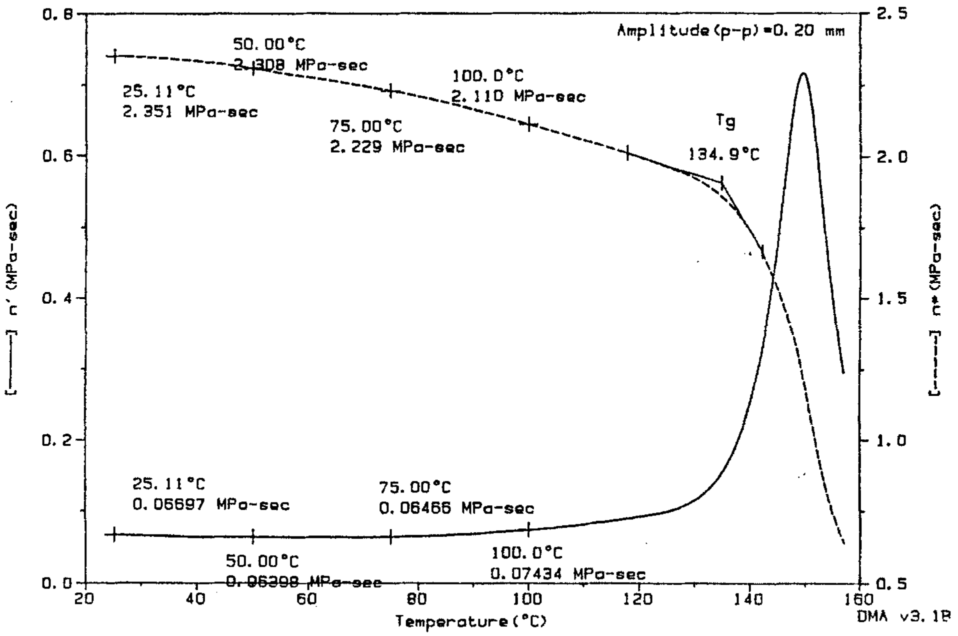

Fig. 5 Dynamic and complex viscosity

Effective density at 50, 75 and 100°C were calculated using the change in the ratio of kinematic to absolute viscosities at these temperatures as shown in Fig. 5 and determined with respect to the known ratio at ambient temperature. This follows from the flow properties of solids at high temperature. The calculated values are given in Table 2.

Table 2

	50°C	75°C	100°C
Density/g cm^{-3}	1.030	1.067	1.288
Diffusivity/cm^2 s^{-1}	1.836×10^{-3}	1.549×10^{-3}	1.193×10^{-3}

Thermal conductivity is found to remain constant with temperature but effective density increases and diffusivity decreases with increasing temperature as a consequence. Variation of density with temperature results from competing effects of densification due to structural rearrangement and thermal expansion. The contribution of thermal expansion appears lower than the densification effect, which results from ordering of molecular chains and shrinkage of free volume in the polymer structure. The actual contribution of thermal expansion to the changes in diffusivity with temperature will be investigated at a future date for this material from determination of stress induced changes in sample temperature. Thermal densification and the resultant degree of ordered state are likely to be responsible for enhanced mechanical strength for this material as evidenced by its engineering applications.

The low level of charging and non-exponential charge dissipation pattern shown in Fig. 6 are characteristics of good insulating materials. Along with the measured capacitance (charge holding capacity) of 164.2 pF @ 60 Hz, Metton LMR can be considered as having a degree of static protection in moving parts applications with respect to charge acquisition and release.

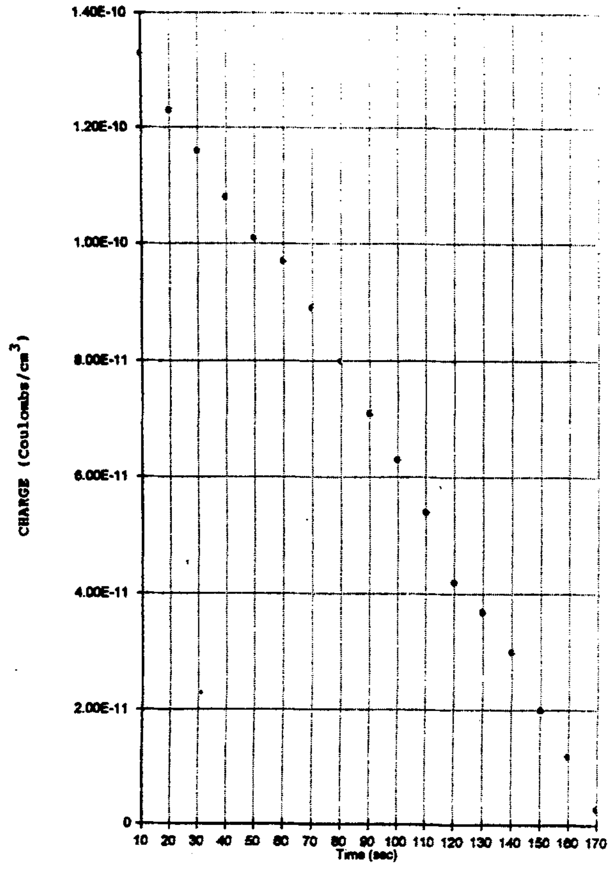

Fig. 6 Static charge decay curve

The dispersion of the short-circuit depolarization (absorption) current occurring between 25 and 190°C is shown in Fig. 7.

The post-T_g rise in current (ρ-peak), which originates from external charging (Maxwell-Wagner effect) [13, 14] confirms the presence of heterogeneous interfaces in Metton, reflecting the binary nature of this material. For further elucidation, thermally stimulated activation energy for the depolarization process, dipole

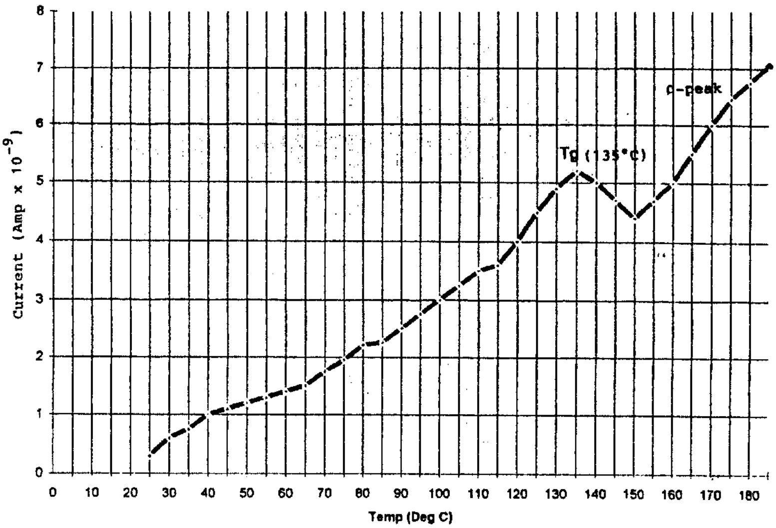

Fig. 7 Thermally stimulated depolarization current

relaxation time, electron drift mobility and electrical conductivity were derived from the initial rise in ohmic conduction between 25 and 130°C as follows:

Activation energy was calculated using the initial rise method of Garlick and Gibson [15] by the relation:

$$\log_e I(T) = C - (\Delta H_a/KT)$$

where I is the depolarization current at temperature T and C is a constant.

Activation energy, ΔH_a, is found by multiplying the slope of the straight line plot of $\log_e I$ *vs.* I/T by the Boltzmann constant, K (in eV/°C).

Dipole relaxation time (τ) at the maximum temperature was calculated by using the equation:

$$\tau = (KT_{max})/H_r\Delta H_a \exp(\Delta H_a/KT_{max})$$

where H_r is the heating rate °C s^{-1} and T_{max} is the maximum temperature at which relaxation time is calculated.

Electron drift mobility, μ_D (in cm^2 V s^{-1}) of charge carriers was calculated by the following equation:

$$\mu_D = J/(NeE)$$

where J is the current density in amp/cm^2, N is the number of charge carriers/cm^3, e is the magnitude of charge on the electron, and E is the field strength in volts/cm.

Electrical conductivity, σ (in $\text{ohm}^{-1}\ \text{cm}^{-1}$) was calculated by the formula:

$$\sigma = Ne\mu_D$$

All calculated values are given in Table 3.

Table 3

T/ °C	Activation energy/eV	τ/ s	μ_D/ $\text{cm}^2(\text{V s})^{-1}$	Conductivity/ $\text{ohm}^{-1}\ \text{cm}^{-1}$
25–50	0.42	1.71×10^{1}	4.43×10^{-6}	4.10×10^{-15}
50–75	0.18	1.17×10^{2}	7.06×10^{-6}	1.70×10^{-14}
75–100	0.16	1.82×10^{2}	9.14×10^{-6}	4.37×10^{-14}

The above values calculated from the depolarization current are reflective of the molecular mobility in the material's structure.

The initial polarization due to applied voltage is brought about by an induced charge shift throughout the material [16] and the discharge current reflects the characteristics of the charging process. The relatively higher activation energy for depolarization at the start of heating is associated with the initial dipole orientation.

The lower activation energies at the higher temperatures suggest low intermolecular cohesion or the presence of shallow trap sites for charge carriers, possibly arising from double bonds or the presence of hetero atoms in the polymer structure. Additional traps are possible from chemical impurities, oxidation products, broken chains and adsorbed molecules [17]. Electrons in such traps require little energy to get into the conduction band and be transported to the discharging electrode under a potential difference. Increase in carrier mobility and hence increased conductivity with temperature confirm low intermolecular cohesion and detrapping from shallow trap levels. These findings along with low activation energy for high temperature depolarization point to the origin of charge carriers from weak secondary bonding typical of polymer interfaces. Increase of relaxation time of trapped carriers with temperature confirms the non-polar nature of this material, according to Debye theory, but may indeed result from electrostatic interaction from charged species in the polarized polymer which demonstrates the utility of Metton's charge storage capacity at higher temperatures. See references [7–10].

The appearance of the T_g-peak at about the expected temperature seems independent of this interaction. No prior data is available for polarization of Metton in stainless steel electrodes.

The mechanism of conduction beyond T_g is related to thermal activation of electrons at the sample/electrode interface. The electrons are injected from the electrodes to the material through inter-electrode space [18, 19] and are not relevant to the present study.

Conclusion

Metton LMR is known to be a strong mechanical performer under ambient conditions. Its rigidity belies its thermo-elasticity at elevated temperatures. This study shows its potential for high level electronic applications requiring static protection, good insulation, low power input and high mobility of charged species.

* * *

The author wishes to acknowledge the assistance provided by Ralph Pitman in the preparation of the samples for this work.

References

1 Hercules Inc., Wilmington, DE, USA.
2 Design and Post-molding Guides by Metton America Inc., 1995.
3 G. L. Wilkes, Adv. Polym. Sci., 8 (1971) 91.
4 TA Instruments, New Castle, DE, USA.
5 Test Protocol EIA-541, Packaging Material Standards for ESD-Sensitive Items.
6 Spellman High Voltage DC Supply, Plainview, New York.
7 J. VanTurnhout, Thermally Stimulated Discharge of Polymer Electrets, Elsevier Scientific, New York 1975.
8 B. Chowdhury, Am. Lab., 17 (1985) 49.
9 B. Chowdhury, Am. Lab., 18 (1986) 28.
10 B. Chowdhury, "Thermally Stimulated Discharge Current Measurement For Thin Polymer Films" in New Characterization Techniques For Thin Polymer Films, Ho-Ming Tong and Luu T. Nguyen, Eds, John Wiley & Sons, Inc., 1990, p. 265.
11 I. Finnie and W. R. Heller, Creep of Engineering Materials, McGraw Hill, New York 1959.
12 D. J. Brown and A. H. Windle, J. Mat. Sci., 19 (1984).
13 J. C. Maxwell, Electricity and Magnetism, Vol. 1, Oxford University Press, London 1892, p. 452.
14 K. W. Wagner, Ann. Phys., 40 (1913) 817.
15 G. F. J. Garlick and A. F. Gibson, Proc. Phys. Soc., 60 (1948) 574.
16 B. Gross, J. Chem. Phys., 17 (1949) 866.
17 J. J. Fuhrmann, J. Electrostat., 4 (1977/78)
18 R. A. Cresswell and M. M. Perlman, J. Appl. Phys., 41 (1970) 2365.
19 B. Gross, G. M. Sessler and J. E. West, J. Appl. Phys., 47 (1976) 968.